# The extent of irregular stress distribution in a two-layer cylindrical bars subjected to the change of temperature

**N. Partaukas\*, J. Bareišis\*\***

*\*Kaunas University of Technology, S. Daukanto St. 12, LT-35212 Panevėžys, Lithuania, E-mail: n.partaukas@gmail.com*
*\*\*Kaunas University of Technology, S. Daukanto St. 12, LT-35212 Panevėžys, Lithuania, E-mail: jonas.bareisis@ktu.lt*

## 1. Introduction

Multi–layer structural elements (MSEs) are made of two or more materials (phases) with different properties and clear boundaries between them. Subjected to external loads the MSEs deform like a single body. MSEs can be considered as hybrid materials, although they differ not only from homogenous, but from composite materials as well. Sometimes MSEs also are referred to as macro–composites.

The major advantage of MSEs is the capacity to obtain new structural properties by varying layers material and their arrangement [1]. Each layer in MSEs serves a specific purpose. The external ones protect from the environmental impact: mechanical damage, moisture and ultraviolet (UV) radiation. The layers from porous materials reduce weight and material consumption. Reinforcement reduces strain, creep and increases strength. The layers limiting the diffusion of liquids and gases, as well as increasing thermal resistance may be also used. Therefore MSEs are employed in different areas [1-3].

The change of temperature in MSEs, the layers of which have different coefficients of thermal expansion (CTE), produce thermal stresses (TS). TS can emerge either during manufacturing processes, or during operation. In each case TS superimpose with stresses from external loads and thus the strength may be impinged [2]. TS can be moderated by selecting materials with similar values of CTE. Since layers in MSEs perform different functions, they are usually made of materials with very different properties: metals, plastics, ceramics and composites. Therefore, TS in MSEs can rarely be eliminated. Consequently, it is essential to be able to estimate and consider TS in MSEs [3].

The free edge effect (FEE), when near at the edge regions stress states are qualitatively and quantitatively different from stresses farther away, manifests itself in MSEs [4, 5]. Often this is the main cause of fracture and delamination [5-7]. Some authors who analyse FEE and stresses in MSE's propose to separate two distinctive zones, namely regular ant irregular ones [1, 4, 8-10]. Sometimes they are also called zones of nominal and anomalous stress distribution. Stresses in regular zone (RZ) along the layer can be considered as constant. In Irregular Zone (IZ), on the contrary they change rapidly, and complex stress/strain state arises [1, 4].

Different methods for the strength and stress assessment in RZ and IZ therefore should be used. Techniques intended for stress estimation in RZ cannot be used even for a rough estimate of the stresses in IZ. Otherwise, not only significant errors arise, but false stress states are portrayed [8-10]. In order to apply such techniques, the extent of IZ should be at least approximately settled, and effecting factors identified.

The objective of the research presented was to examine the extent of IZ in a solid, two-layer, cylindrical bars subjected to the change of temperature, to assess the boundaries of its variation, determine the dominant factors, and find a set of parameters which are intrinsic for the bars with a long IZ and a short one.

## 2. Methods

In experimental terms strains inside MSEs can by examined by means of strain gages (SG). The gage length can be as small as a couple of tenths of millimetres, so they can be used in research of FEE in MSEs [11, 12]. However, this method is not very attractive for the research of IZ extent. Firstly, in order to evaluate the influence of various factors and their possible interactions a couple of dozens of different combinations should be examined (Eq. (1)). Since strains in each sample should be measured at a couple of points, experimental approach quickly will become cost ineffective and time consuming. On the other hand, the SG and their wiring will have influence on strains, especially when the values of the Young's modulus are low [13]. Uncertainties due temperature, transvers sensitivity of SG and other effects should be estimated.

Other experimental techniques cannot be used for strain measurement inside of material or if they are, strains are obtained in a relatively large (in order of centimetres) basis [14]. Measurement of strains at the external surface of MSEs is not a good recourse, either. Delamination and fracture usually starts at the contact of the layers, so strains at the external surface would not be very expedient [15]. Regarding this state of affairs, the method of finite elements (FEM) as a convenient tool for research on the extent of IZ is adopted.

The geometry of the layered bar and corresponding FEM model in Fig. 1 are presented. The length of the bar $L$ was taken as equal to four diameters $D$ i.e. $L = 4D$. The mesh was generated in such a way that no less than 200 of finite elements along the distance of one diameter would be assured (Fig. 1). Plane four node elements with the option of axial symmetry were used (Plane 182). Finite elements at a contact surface were bonded together without a slip. Materials were considered as homogeneous, isotropic and linearly elastic. Constrains which we used for a model are presented in Fig. 1. The load which induces TS was the change in layers temperature ($\Delta T = 1$ºC). Simulation was performed by FEA software package Ansys 13.
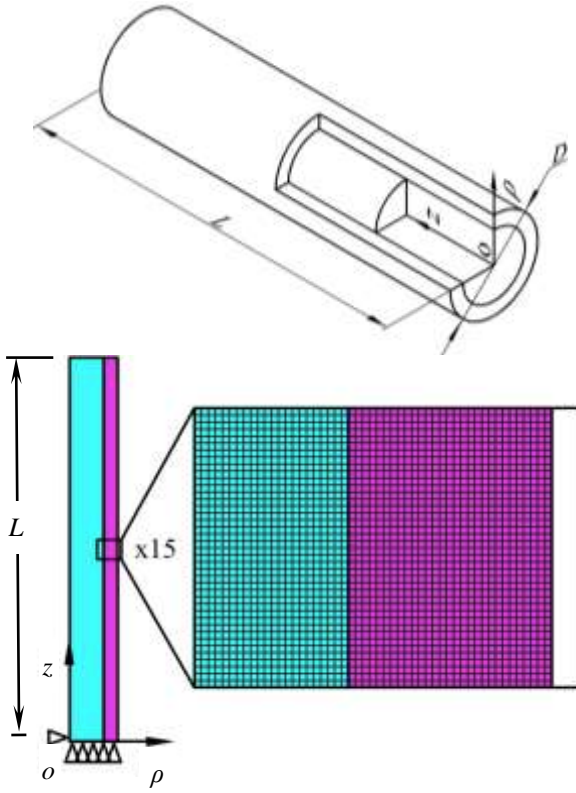
Fig. 1 The geometry (top) and corresponding FEM model (bottom) of the two-layer bar

It can be suspected that the length of irregular stress distribution (IZ) will be influenced by mechanical properties, like Young's modulus $E_i$, Poison's ratio $v_i$ and by geometry of the layers. To estimate the influence of the latter, the ratio of the areas of layers $A_i$ and MSEs $A$ cross–sections were used $\psi_i = A_i/A$. The difference between CTE of the layers $\alpha_i$ was $\alpha_2 - \alpha_1 = 1 \cdot 10^{-6}$ 1/°C. While thermal strains are proportional to the change in temperature, TS induced in MSEs are proportional to the difference in CTE of the layers. So TS in MSE's with different values of CTE's can be easily recalculated.

Young's modulus of the two–layer MSEs can be represented by one parameter, namely with a ratio between them $\xi_{2,1} = E_2/E_1$. Therefore, TS and the extent of irregular stress distribution will depend on five parameters of the bar: $\xi_{2,1}, \psi_1, \psi_2, v_1, v_2$. For the two–layer bars $\psi_2 = 1 - \psi_1$, therefore, the influence of four independent parameters was analysed. The total number of trials required to implement a Full Factorial Design (FFD) is:

$$N = r\prod_{j=1}^{S} q_j = r\,3^4 = 81\,r, \tag{1}$$

where $r$ is the number of replicates, $S$ is the number of different factors, $q_j$ is the number of levels in $j$-th factor.

Since FEM in its nature is a deterministic one, it is sufficient to take only one replicate $r = 1$. For that same reason the order of the specimen's simulations was not randomized.

The simulations were carried out with the following levels of parameters: $\xi_{2,1}$ (0.1, 1.0, 10.0); $\psi_1$ (0.1, 0.5, 0.9); $v_1$ (0.19, 0.34, 0.49); $v_2$ (0.19, 0.34, 0.49). By increasing the number of levels, the number of tests raises drastically (Eq. (1)).

Usually two–level experimental designs with "high" and "low" values of each parameter are used [16, 17]. Here we are interested in those cases, where corresponding parameters between the layers are equal, as well. Therefore, the factorial design where each parameter has three levels was used, even if the total number of trials in comparison to the two-level design were approximately 5 times higher. Three level designs also enable to estimate the nonlinearity effects.

The range of each parameter variation was selected as quite wide in order to get clear differences between the levels. The limit values of parameters $\psi_1$ and $v_i$ were chosen near to the maximum possible.

To define the length of IZ ($L^{IZ}$) the range of stress variation $|\sigma_{max} - \sigma_{min}|$ and coefficient $k$ were used (Fig. 2). Here we take $k$ equal to 5 per cent. Stress variation in 5% is quoted as small to assume that the stresses in that region are constant.
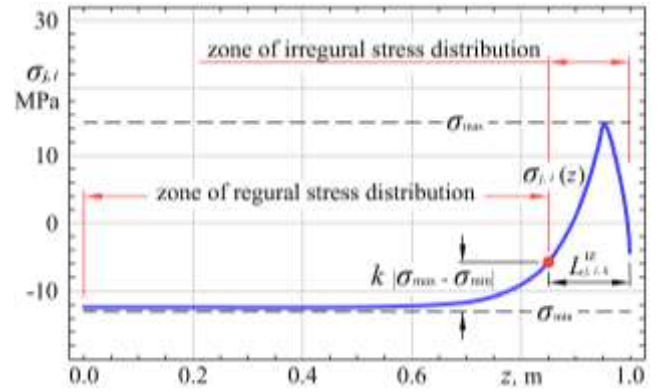


Fig. 2 Separation between the zones of regular and irregular stress distribution

IZ defined in such a way can be applied even when the stresses in the zone of regular stress distribution are equal to zero. On the other hand, this definition estimates not only the stress change from its maximal value ($\sigma_{max}$), but its change in comparison to the stress variation.

It can be noted that when $k = 100$ %, $L^{IZ}$ is equal to the length of the maximal stress value from the end of the bar. When $k = 0$ %, $L^{IZ}$ is equal to length of the bar ($L$). The values of the stresses along the axis $0z$ was obtained by Ansys command PATH.

The length of IZ was defined as a ratio:

$$\Phi_{j,i}^k = \frac{L_{j,i,k}^{IZ}}{D}, \tag{2}$$

where $j$ denotes the component of the stress state; $i$ is the number of the layer.

## 3. Results

The results of IZ calculated by means of FEM are presented in Table 1. In the columns denoted "Code" factors and their levels are encoded. Numbers 1, 2 and 3 correspondingly signify the "low", "medium" and "high" values of each parameter. The numbers in the first and second positions encode the ratios of Young's modulus and layers cross–sectional areas. The numbers in the third and last positions indicate the values of Poisson's ratio in the inter-

nal and external layers. For example, the code 1231 represents the construction where: $\xi_{2,1} = 0.1$, $\psi_1 = 0.5$, $v_1 = 0.49$, $v_2 = 0.19$. In each row, the values of the IZ lengths $\Phi$ for

different components of the stress state are given: normal (along $or$, $o\theta$ and $oz$ directions), shear $\tau$ and von Mises $e$.

Table

The extent of irregular stress distribution

| Code | $\Phi_{r,1}$ | $\Phi_{\theta,1}$ | $\Phi_{z,1}$ | $\Phi_{\tau,1}$ | $\Phi_{e,1}$ | $\Phi_{r,2}$ | $\Phi_{\theta,2}$ | $\Phi_{z,2}$ | $\Phi_{\tau,2}$ | $\Phi_{e,2}$ | Code | $\Phi_{r,1}$ | $\Phi_{\theta,1}$ | $\Phi_{z,1}$ | $\Phi_{\tau,1}$ | $\Phi_{e,1}$ | $\Phi_{r,2}$ | $\Phi_{\theta,2}$ | $\Phi_{z,2}$ | $\Phi_{\tau,2}$ | $\Phi_{e,2}$ |
|---|---|---|---|---|---|---|---|---|---|---|---|---|---|---|---|---|---|---|---|---|---|
| 1111 | 0.80 | 0.88 | 1.16 | 1.04 | 1.04 | 0.80 | 0.80 | 0.96 | 1.04 | 1.00 | 2231 | 0.52 | 0.72 | 0.80 | 0.64 | 0.64 | 0.52 | 0.76 | 0.64 | 0.64 | 0.72 |
| 1112 | 0.76 | 0.84 | 1.28 | 1.08 | 1.08 | 0.76 | 0.52 | 0.84 | 1.08 | 0.96 | 2232 | 0.44 | 0.76 | 0.88 | 0.68 | 0.68 | 0.40 | 0.76 | 0.76 | 0.68 | 0.80 |
| 1113 | 0.68 | 0.80 | 1.36 | 1.12 | 1.12 | 0.68 | 0.28 | 0.76 | 1.12 | 0.84 | 2233 | 0.24 | 0.80 | 0.96 | 0.72 | 0.72 | 0.24 | 0.80 | 0.96 | 0.72 | 0.88 |
| 1121 | 0.80 | 0.96 | 1.16 | 1.04 | 1.04 | 0.80 | 0.96 | 0.96 | 1.04 | 1.00 | 2311 | 0.16 | 0.76 | 0.48 | 0.40 | 0.40 | 0.32 | 0.76 | 0.48 | 0.36 | 0.64 |
| 1122 | 0.72 | 0.96 | 1.24 | 1.08 | 1.08 | 0.72 | 0.72 | 0.84 | 1.08 | 0.92 | 2312 | 0.44 | 0.80 | 0.52 | 0.44 | 0.44 | 0.52 | 0.72 | 0.52 | 0.40 | 0.64 |
| 1123 | 0.64 | 1.00 | 1.36 | 1.12 | 1.12 | 0.60 | 0.24 | 0.76 | 1.12 | 0.80 | 2313 | 0.56 | 0.84 | 0.52 | 0.44 | 0.44 | 0.68 | 0.68 | 0.56 | 0.44 | 0.64 |
| 1131 | 0.76 | 1.08 | 1.12 | 1.00 | 1.00 | 0.76 | 1.08 | 0.96 | 1.04 | 1.00 | 2321 | 0.16 | 0.64 | 0.48 | 0.36 | 0.36 | 0.16 | 0.72 | 0.48 | 0.36 | 0.60 |
| 1132 | 0.72 | 1.20 | 1.24 | 1.04 | 1.04 | 0.68 | 0.84 | 0.84 | 1.08 | 0.88 | 2322 | 0.44 | 0.64 | 0.48 | 0.40 | 0.40 | 0.48 | 0.64 | 0.48 | 0.36 | 0.60 |
| 1133 | 0.56 | 1.12 | 1.36 | 1.08 | 1.08 | 0.48 | 0.48 | 0.76 | 1.12 | 0.76 | 2323 | 0.52 | 0.68 | 0.52 | 0.44 | 0.44 | 0.64 | 0.64 | 0.52 | 0.40 | 0.60 |
| 1211 | 0.56 | 0.68 | 0.48 | 0.60 | 0.60 | 0.52 | 0.60 | 0.56 | 0.60 | 0.56 | 2331 | 0.28 | 0.52 | 0.44 | 0.32 | 0.32 | 0.16 | 0.64 | 0.44 | 0.32 | 0.56 |
| 1212 | 0.52 | 0.68 | 0.44 | 0.64 | 0.64 | 0.52 | 0.60 | 0.64 | 0.64 | 0.44 | 2332 | 0.40 | 0.56 | 0.44 | 0.36 | 0.36 | 0.40 | 0.60 | 0.44 | 0.32 | 0.56 |
| 1213 | 0.48 | 0.72 | 0.40 | 0.68 | 0.68 | 0.48 | 0.56 | 0.56 | 0.68 | 0.28 | 2333 | 0.52 | 0.56 | 0.48 | 0.40 | 0.40 | 0.56 | 0.56 | 0.48 | 0.36 | 0.56 |
| 1221 | 0.52 | 0.68 | 0.44 | 0.56 | 0.56 | 0.52 | 0.60 | 0.56 | 0.56 | 0.56 | 3111 | 0.32 | 0.56 | 0.44 | 0.36 | 0.36 | 0.32 | 0.64 | 0.48 | 0.36 | 0.56 |
| 1222 | 0.52 | 0.72 | 0.44 | 0.60 | 0.60 | 0.52 | 0.60 | 0.60 | 0.60 | 0.48 | 3112 | 0.32 | 0.60 | 0.48 | 0.36 | 0.36 | 0.32 | 0.60 | 0.48 | 0.36 | 0.44 |
| 1223 | 0.48 | 0.76 | 0.40 | 0.64 | 0.64 | 0.48 | 0.56 | 0.56 | 0.68 | 0.32 | 3113 | 0.32 | 0.64 | 0.52 | 0.36 | 0.36 | 0.32 | 0.24 | 0.48 | 0.36 | 0.24 |
| 1231 | 0.52 | 0.64 | 0.44 | 0.56 | 0.56 | 0.52 | 0.60 | 0.52 | 0.56 | 0.56 | 3121 | 0.36 | 0.28 | 0.40 | 0.40 | 0.40 | 0.36 | 0.72 | 0.48 | 0.44 | 0.68 |
| 1232 | 0.52 | 0.64 | 0.40 | 0.60 | 0.60 | 0.52 | 0.60 | 0.60 | 0.60 | 0.48 | 3122 | 0.36 | 0.28 | 0.40 | 0.40 | 0.40 | 0.36 | 0.68 | 0.48 | 0.44 | 0.68 |
| 1233 | 0.48 | 0.68 | 0.36 | 0.64 | 0.64 | 0.48 | 0.56 | 0.52 | 0.64 | 0.32 | 3123 | 0.36 | 0.28 | 0.40 | 0.40 | 0.40 | 0.36 | 0.64 | 0.48 | 0.44 | 0.64 |
| 1311 | 0.12 | 0.56 | 0.36 | 0.16 | 0.16 | 0.12 | 0.44 | 0.32 | 0.12 | 0.36 | 3131 | 0.48 | 0.44 | 0.48 | 0.60 | 0.60 | 0.48 | 0.76 | 0.48 | 0.60 | 0.68 |
| 1312 | 0.12 | 0.60 | 0.36 | 0.16 | 0.16 | 0.12 | 0.36 | 0.32 | 0.16 | 0.44 | 3132 | 0.48 | 0.44 | 0.48 | 0.60 | 0.60 | 0.48 | 0.80 | 0.44 | 0.60 | 0.72 |
| 1313 | 0.12 | 0.64 | 0.36 | 0.20 | 0.20 | 0.12 | 0.36 | 0.32 | 0.16 | 0.52 | 3133 | 0.48 | 0.44 | 0.48 | 0.60 | 0.60 | 0.48 | 0.88 | 0.44 | 0.60 | 0.76 |
| 1321 | 0.08 | 0.44 | 0.36 | 0.16 | 0.16 | 0.12 | 0.40 | 0.32 | 0.12 | 0.32 | 3211 | 0.80 | 0.76 | 0.48 | 0.72 | 0.72 | 0.76 | 0.80 | 0.88 | 0.72 | 0.80 |
| 1322 | 0.12 | 0.44 | 0.36 | 0.16 | 0.16 | 0.12 | 0.32 | 0.32 | 0.16 | 0.40 | 3212 | 0.76 | 0.72 | 0.52 | 0.76 | 0.76 | 0.76 | 0.80 | 0.88 | 0.76 | 0.80 |
| 1323 | 0.12 | 0.48 | 0.36 | 0.20 | 0.20 | 0.12 | 0.32 | 0.32 | 0.16 | 0.48 | 3213 | 0.76 | 0.72 | 0.60 | 0.76 | 0.76 | 0.72 | 0.80 | 0.84 | 0.76 | 0.84 |
| 1331 | 0.08 | 0.36 | 0.32 | 0.16 | 0.16 | 0.12 | 0.36 | 0.32 | 0.12 | 0.24 | 3221 | 0.76 | 0.64 | 0.48 | 0.80 | 0.80 | 0.76 | 0.88 | 0.96 | 0.76 | 0.92 |
| 1332 | 0.08 | 0.40 | 0.36 | 0.16 | 0.16 | 0.12 | 0.28 | 0.28 | 0.12 | 0.36 | 3222 | 0.76 | 0.60 | 0.56 | 0.80 | 0.80 | 0.76 | 0.88 | 0.96 | 0.80 | 0.96 |
| 1333 | 0.08 | 0.40 | 0.36 | 0.16 | 0.16 | 0.12 | 0.28 | 0.28 | 0.16 | 0.48 | 3223 | 0.76 | 0.32 | 0.60 | 0.80 | 0.80 | 0.76 | 0.92 | 0.96 | 0.80 | 0.96 |
| 2111 | 0.68 | 0.72 | 0.64 | 0.60 | 0.60 | 0.68 | 0.72 | 0.64 | 0.60 | 0.28 | 3231 | 0.88 | 0.56 | 0.68 | 0.96 | 0.96 | 0.88 | 1.08 | 1.28 | 0.96 | 1.08 |
| 2112 | 0.68 | 0.72 | 0.68 | 0.60 | 0.60 | 0.64 | 0.60 | 0.64 | 0.60 | 0.40 | 3232 | 0.88 | 0.64 | 0.72 | 1.00 | 1.00 | 0.88 | 1.16 | 1.32 | 0.96 | 1.16 |
| 2113 | 0.68 | 0.72 | 0.76 | 0.60 | 0.60 | 0.64 | 0.28 | 0.60 | 0.60 | 0.44 | 3233 | 0.92 | 0.72 | 0.80 | 1.00 | 1.00 | 0.92 | 0.92 | 0.92 | 0.92 | 0.92 |
| 2121 | 0.60 | 0.68 | 0.56 | 0.56 | 0.56 | 0.56 | 0.76 | 0.64 | 0.56 | 0.52 | 3311 | 0.88 | 0.84 | 0.80 | 0.80 | 0.80 | 0.84 | 0.88 | 0.84 | 0.80 | 0.88 |
| 2122 | 0.56 | 0.68 | 0.64 | 0.60 | 0.60 | 0.56 | 0.68 | 0.64 | 0.60 | 0.28 | 3312 | 0.84 | 0.84 | 0.80 | 0.84 | 0.84 | 0.84 | 0.92 | 0.88 | 0.84 | 0.92 |
| 2123 | 0.56 | 0.72 | 0.72 | 0.60 | 0.60 | 0.52 | 0.52 | 0.60 | 0.60 | 0.40 | 3313 | 0.84 | 0.80 | 0.80 | 0.88 | 0.88 | 0.84 | 0.92 | 0.92 | 0.84 | 0.96 |
| 2131 | 0.52 | 0.68 | 0.48 | 0.56 | 0.56 | 0.52 | 0.76 | 0.64 | 0.56 | 0.40 | 3321 | 0.80 | 0.88 | 0.80 | 0.80 | 0.80 | 0.76 | 0.92 | 0.80 | 0.76 | 0.96 |
| 2132 | 0.24 | 0.68 | 0.56 | 0.56 | 0.56 | 0.24 | 0.76 | 0.64 | 0.56 | 0.44 | 3322 | 0.80 | 0.88 | 0.80 | 0.80 | 0.80 | 0.80 | 0.96 | 0.84 | 0.80 | 0.96 |
| 2133 | 0.24 | 0.68 | 0.64 | 0.60 | 0.60 | 0.24 | 0.68 | 0.64 | 0.60 | 0.16 | 3323 | 0.80 | 0.84 | 0.84 | 0.88 | 0.88 | 0.80 | 1.00 | 0.92 | 0.84 | 1.00 |
| 2211 | 0.56 | 0.76 | 0.96 | 0.72 | 0.72 | 0.56 | 0.76 | 0.96 | 0.72 | 0.80 | 3331 | 0.72 | 0.84 | 0.76 | 0.76 | 0.76 | 0.72 | 0.92 | 0.76 | 0.72 | 0.88 |
| 2212 | 0.48 | 0.76 | 0.88 | 0.76 | 0.76 | 0.20 | 0.76 | 0.88 | 0.76 | 0.80 | 3332 | 0.76 | 0.88 | 0.80 | 0.80 | 0.80 | 0.72 | 0.92 | 0.80 | 0.76 | 0.92 |
| 2213 | 0.24 | 0.76 | 0.36 | 0.80 | 0.80 | 0.24 | 0.72 | 0.76 | 0.80 | 0.76 | 3333 | 0.76 | 0.88 | 0.84 | 0.84 | 0.84 | 0.76 | 0.96 | 0.88 | 0.84 | 0.96 |
| 2221 | 0.56 | 0.76 | 0.88 | 0.68 | 0.68 | 0.52 | 0.76 | 0.80 | 0.68 | 0.84 | Q-1 | 0.35 | 0.60 | 0.44 | 0.40 | 0.40 | 0.32 | 0.59 | 0.48 | 0.43 | 0.47 |
| 2222 | 0.44 | 0.76 | 0.96 | 0.72 | 0.72 | 0.20 | 0.76 | 0.96 | 0.72 | 0.84 | Q-2 | 0.52 | 0.72 | 0.52 | 0.60 | 0.60 | 0.52 | 0.72 | 0.64 | 0.60 | 0.68 |
| 2223 | 0.24 | 0.80 | 0.84 | 0.76 | 0.76 | 0.24 | 0.76 | 0.84 | 0.76 | 0.84 | Q-3 | 0.76 | 0.80 | 0.80 | 0.80 | 0.80 | 0.72 | 0.80 | 0.84 | 0.80 | 0.88 |

*Notes:* The extent of IZ is obtained by using $k = 5\%$; blue colour denotes „short", green and pink respectively „medium" and „long" IZ.

From Table we see that the length of IZ varies from 0.08 to 1.36, or approximately from 0.1 to 1.4 of the external diameter $D$ of the bar. The ratio between the shortest and longest IZ is equal to 17, i.e. differs approximately 20 times. That is a very large variation, so it is important to determine the underlying causes.

By examining the results presented (Table), we see that the extents of IZ are distributed unevenly. To estimate the scattering of the results, quartiles $Q$ instead of standard deviation were used as a less affected by outliers (robust statistics). Considering the values of the first $Q$–1 and the third $Q$–3 quartiles, we define the length of IZ as

„short", when $\Phi < 0.4$ and „long", when $\Phi > 0.8$, for the axial, shear and von Mises stresses. For the stresses in radial direction those limits are 0.33 and 0.73 and for the hoop stresses they are correspondingly 0.6 and 0.8.

Marking "short", "medium" and "long" IZ by different colours (Table) we see that there is no clear distinction between those three cases. Short IZ usually are obtained in the bars with codes " 31_ _" (here instead of each dash any of numbers 1, 2 or 3 can be used) and long in with codes "33_ _". A clear trend towards the long IZ shows in bars "11_ _" and in less extent in bars "32_ _". While bars "21_ _" and "12_ _" can be considered as having medium lengths of IZ.
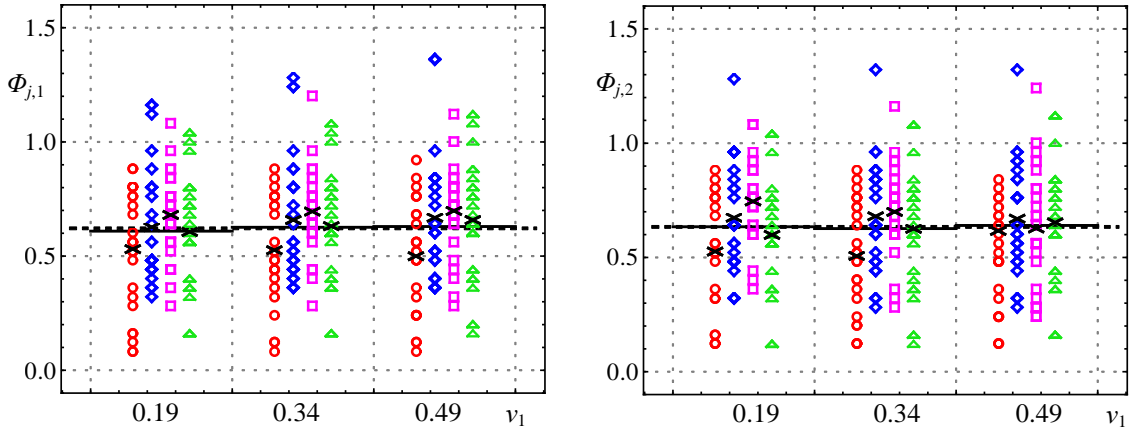
Fig. 3 The extent of IZ in internal (left) and external (right) layers with the different values of Poisson's ratios: $\circ - \Phi_{r,i}$, $\square - \Phi_{\theta,i}$, $\triangle - \Phi_{\tau,i}$, $\lozenge\ \Phi_{e,i}$
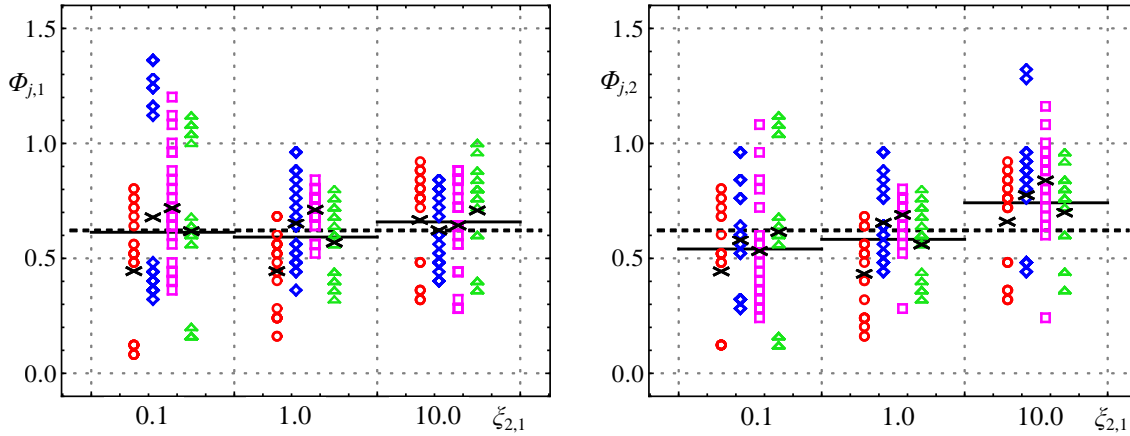


Fig. 4 The extent of IZ in internal (left) and external (right) layers with the different values of ratios of Young's modulus: $\circ - \Phi_{r,i}$, $\square - \Phi_{\theta,i}$, $\triangle - \Phi_{\tau,i}$, $\lozenge\ \Phi_{e,i}$
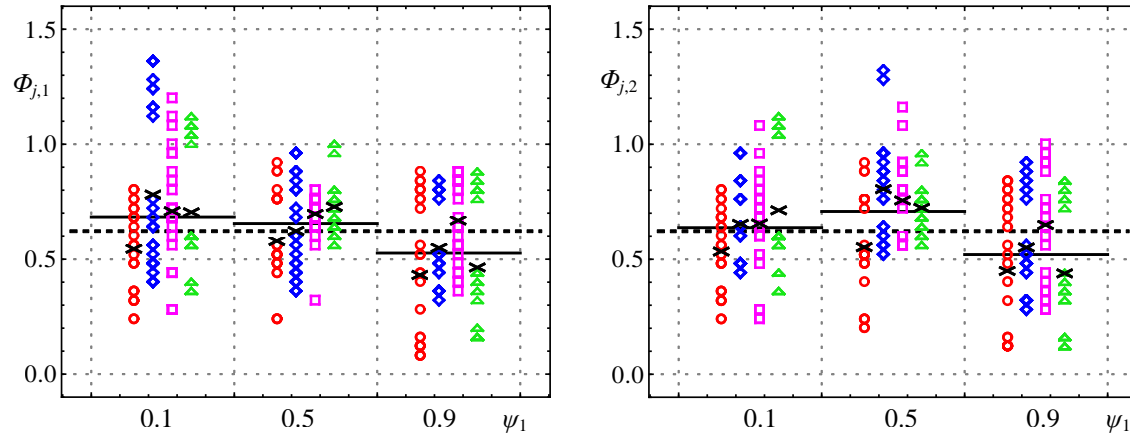


Fig. 5 The extent of IZ in internal (left) and external (right) layers with the different values of areas cross-sections: $\circ - \Phi_{r,i}$, $\square - \Phi_{\theta,i}$, $\triangle - \Phi_{\tau,i}$, $\lozenge\ \Phi_{e,i}$

An interesting distribution can be observed in bars encoded "22_ _". Here "short", "medium" or even "long" IZ can be obtained. Obviously, the extent of IZ in this case strongly depends on the values of Poisson's ratios or their interaction with the ratios of Young's modulus and the layers cross–sectional areas. However, this is more likely an exception than a rule, since in all the other cases the values of Poisson's ratios has very little effect on IZ (Fig. 3). In Figs. 3-5 the black–dashed line signifies the average of all the results in Table (equal to 0.63$D$). The black solid lines signify the averages within each group. X marks denote the average of IZ in each stress component. It should be noted that in Figs. 3-5 the variables in horizontal axis are discrete, not continuing.

Although the average lengths of IZ between the groups with different values of Poisson's ratios are insignificant, the differences in data scattering are noticeable (Fig. 3). This means that the influence of Poisson's ratios to the extent of IZ manifests itself in interaction with $\xi_{2,1}$ and $\psi_1$. Despite of this, the stress state in some loading conditions can be affected by Poisson's ratios [18, 19].
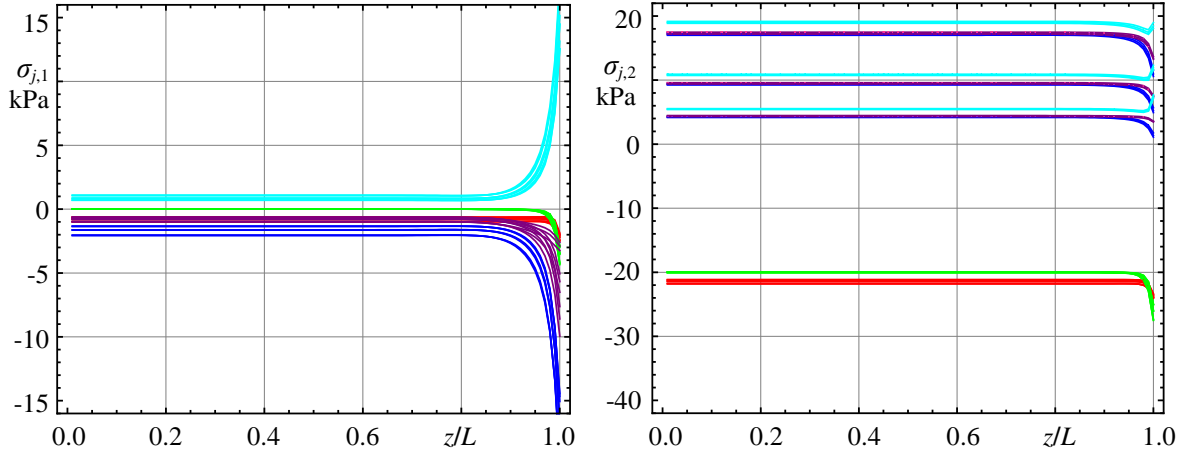
Fig. 6 Stress distribution along the axis in bars „13_ _" at the internal (left) and external (right) layers: $\sigma_{r,i}$, $\sigma_{z,i}$, $\sigma_{\theta,i}$, $\tau$, $\sigma_{e,i}$
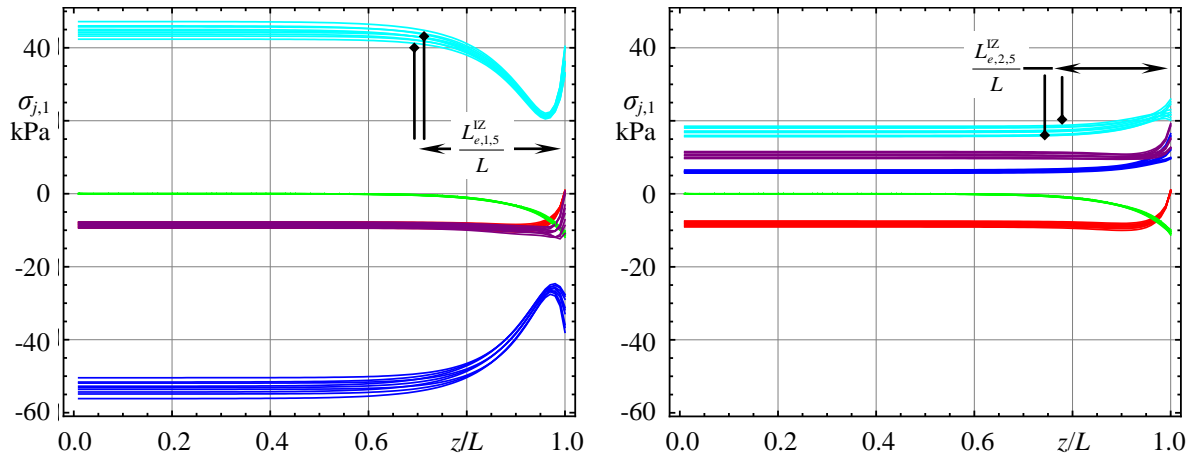


Fig. 7 Stress distribution along the axis in bars „11_ _" at the internal (left) and external (right) layers: $\sigma_{r,i}$, $\sigma_{z,i}$, $\sigma_{\theta,i}$, $\tau$, $\sigma_{e,i}$

The influence of Young's modulus and the areas of layers cross–sections are much more pronounced (Figs. 4 and 5). These graphs also show that the length of IZ depends not only on the Young's modulus and the ratios of area cross–sections (average), but also on their interactions (variation).

In general, referring to the previous results we can suggest that when the values of Young's modulus and ratio of cross–sectional areas are simultaneously relatively high or low (in comparison with another layer). IZ tends to be short (13_ _, 31_ _). Similarly, those zones are short if Young's modules are similar and the cross–sectional area of the internal layer is much higher than that of the internal one (23_ _). The longest IZs are obtained when Young's modulus of the internal layer is relatively high and the cross–sectional area small (11_ _). Similarly IZs are long when Young's modulus of the internal layer is low and the cross–sectional areas are similar or higher than that of the external one (32_ _, 33_ _).

If Young's modulus and the cross–sectional areas of both layers are similar, then the extent of IZ varies quite widely (22_ _). When the internal layer is stiff (high $E_1$) and the cross–sectional area is similar to the external one, we arrive to the IZ with a moderate length (12_ _). Likewise IZ are moderate if Young's moduli are similar, but the cross–sectional area of the internal layer is relatively small (21_ _). The stress distribution along the bar axis at the layers contact for the bars with long and short IZ's are presented respectively in Figs. 6 and 7.

## 4. Discussion

As we see from Table, the extent of irregular stress distribution for radial stresses in both layers are not identical. This is also true and for shear stresses. Those differences can be explained in part by the uncertainty of FEM, in part by the fact that the stresses were taken by a small distance (0.01% of contact surface radius) away from the contact between the layers, to avoid averaging effect.

In the previous section some recommendations for forecasting of the extent of IZ were given. Let's examine how accurate they are. For the lack of space, let us consider only the lengths of normal stresses in the axial direction ($oz$) i.e. $\Phi_{z,i}$. All 81 constructions were subdivided into four categories. The bars with "long", "moderate", "short" and "unstable" lengths of IZ as a box–whisker plots are presented (Fig. 8). Here the plus sign signifies the outliers.

From Fig. 8 we see that the guidance given is not very accurate, since some overlap exist. However, they can serve as a rough estimation for the extent of IZ quite well. By using them we can predict how wide the irregular zone will be before obtaining the actual TS acting in MSEs layers.
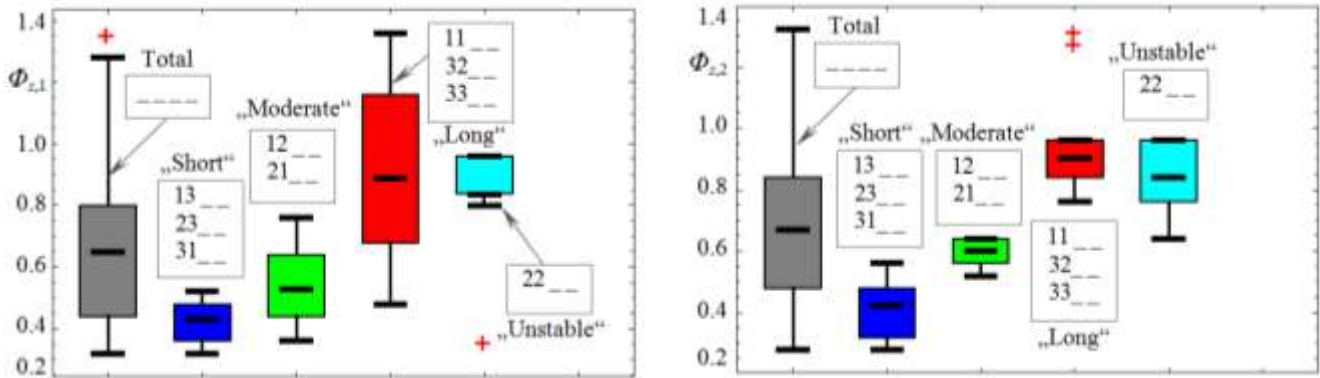
Fig. 8 The box–whisker plots of $\Phi_{z,i}$ of internal (left) and external (right) layers for normal stresses in the axial direction

## 4. Conclusions

1. Examination of thermal stresses in two–layered cylindrical bars, induced demonstrated that stresses varies along its axis. The stress distribution can be arbitrary separated in two distinctive parts, namely regular and irregular stress distribution zones. In regular stress distribution zone stresses can be considered as invariable along the axis.

2. By analysing results from 81 structures with a different values of Young's modulus, Poisson's ratios and cross–sectional ratios of the layers was founded, that the length of IZ for separate stress components are different. It varies from $0.1D$ to $1.4D$. By average the longest IZ was obtained for hoop and axial stresses $0.7D$, ranging from $0.3D$ to $1.4D$. The shortest IZ was attained for radial stresses with average $0.5D$, varying from $0.1D$ to $0.9D$. The total average of all results vas equal to $0.6D$.

3. Presented results indicates that extent of the IZ is most affected by values of Young's modulus and cross-sectional areas of the layers. The influence of Poisson's ratios manifests itself only in interaction with those parameters. Therefore if all parameters remain fixed, except the Poisson's ratios of the layers, the extent of IZ remains practically unaltered.

4. Based on presented results we proposed all layered bars arbitrary subdivide in to four different groups. Each of them can be characterized as hawing "long", "moderate", "short" or "unstable" length of IZ. When the values of Young's modulus and ratio of cross–sectional areas are simultaneously relatively high or low. IZ tends to be short. Similarly, those zones are short if Young's modules are similar and the cross–sectional area of the internal layer is much higher than that of the internal one. The longest IZ are obtained when Young's modulus of the internal layer is relatively high and the cross–sectional area small. Similarly IZ are long when Young's modulus of the internal layer is low and the cross–sectional areas are similar or higher than that of the external one. If Young's modulus and the cross–sectional areas of both layers are similar, then the extent of IZ varies quite widely. When the internal layer is stiff and the cross–sectional area is similar to the external one, we arrive to the IZ with a moderate length. Likewise IZ are moderate if Young's moduli are similar, but the cross–sectional area of the internal layer is relatively small.

5. In bars with "long" IZ parameter $\Phi$ varies from 0.24 to 1.36 with average 0.86. Similarly for those with "short" IZ varies from 0.08 to 0.88 and average 0.41. For those attributed to "moderate" IZ length respectively 0.16, 0.76 and 0.57.

## References

1. **Bareišis, J.** 2006. Strength of Plastics, Composites and Multi-layered Structural Elements. – Kaunas: Technologija, 252p. (in Lithuanian).

2. **Parlevliet P.; Bersee H.; Beukers, A.** 2006. Residual stresses in thermoplastic composites – a study of the literature–Part I: Formation of residual stresses. – composites Part A: Applied Science and Manufacturing 37(11): 1847-1857.
http://dx.doi.org/10.1016/j.compositesa.2005.12.025.

3. **Parlevliet, P.; Bersee, H.; Beukers, A.** 2007.Residual stresses in thermoplastic composites – a study of the literature–Part III: Effects of thermal residual stresses. – composites Part A: Applied Science and Manufacturing 38(6): 1581-1596.
http://dx.doi.org/10.1016/j.compositesa.2006.12.005.

4. **Bareišis ,J.; Garuckas, D.** 2000. stress state of multi-layered structural elements subjected to static loading and optimisiation of laminated beams and bars, Mechanins of Composite Materials 36(5): 153-164.
http://dx.doi.org/10.1023/A:1026638915553.

5. **Panigrahi, S.K.; Pradhan, B.** 2007. Delamination damage analyses of adhesively bonded lap shear joints in laminated FRP composites, International Journal of Fracture 148(4): 373-385.
http://dx.doi.org/10.1007/s10704-008-9210-x.

6. **Adams, M.E.; Campbell, G.A.; Cohen, A.** 1991. Thermal stress induced damage in a thermoplastic matrix material for advanced composites, Polymer Engineering and Science 31(18): 1337-1343.
http://dx.doi.org/10.1002/pen.760311808.

7. **Samyn, P.** et al. 2006. Fracture assessment of carbon fibre/epoxy reinforcing rings through a combination of full-scale testing, small-scale testing and stress modelling, Applied Composite Materials, vol. 13, no. 2, p. 57-85.
http://dx.doi.org/10.1007/s10443-006-9007-x.

8. **Partaukas, N.** 2012. Research on Stress State and Strength in Multilayer Bars and Pipes. Summary of Doctoral Dissertation, Kaunas Univ. of Technology, Kaunas.

9. **Partaukas, N.; Bareišis, J.** 2012. Numerical analysis of free edge effect in out–of–plane loaded sandwiches, Mechanika 2012: 17th International Conference, April 12-13, Kaunas, Lithuania, 218-223.

10. **Partaukas, N.; Bareišis, J.** 2012. Temperature induced stresses in two-phase rectangular macro–composites.

ITELMS 2012: 7th International Conference, May 03-04, Panevėžys, Lithuania, 135-140.

11. **Murray, W.M.; Miller, W.R.** 1992. The Bonded Electrical Resistance Strain Gage. – Oxford University Press: New York, 409p.

12. Vishay: General Purpose Strain Gages – Linear Pattern, (Document Number: 11069), Vishay Micro-Measurements, Raleigh, 2010.

13. **Ajovalasit, A.; Zuccarello, B.** 2007. Stiffness and reinforcement effect of electrical resistance strain gauges, Strain 43(4): 299-305.
http://dx.doi.org/10.1111/j.1475-1305.2007.00354.x.

14. **Sharpe, W.N.** 2008. Springer Handbook of Experimental Solid Mechanics. – Berlin: Springer, 1097p.
http://dx.doi.org/10.1007/978-0-387-30877-7.

15. **Lagunegrand L.,** et al. 2006. Initiation of free-edge delamination in composite laminates. Composites Science and Technology 6(10): 1315-1327.
http://dx.doi.org/10.1016/j.compscitech.2005.10.010.

16. **Mee, R.W.** 2009. A Comprehensive Guide to Factorial Two–Level Experimentation. – Dordrecht: Springer, 549p.
http://dx.doi.org/10.1007/b105081.

17. **Hinkelmann, K.; Kempthorne, O.** 2008. Design and Analysis of Experiments, Vol.1 – Hoboken: Wiley-Interscience, 631p.

18. **Partaukas, N.; Bareišis, J.** 2011. Poisson's ratios influence on strength and stiffness of cylindrical bars, Mechanika 17(2): 132-138.
http://dx.doi.org/10.5755/j01.mech.17.2.327.

19. **Partaukas, N.; Bareišis, J.** 2009. The stress state in two-layer hollow cylindrical bars, Mechanika 15(1): 5-12.

N. Partaukas, J. Bareišis

IREGULIARINĖS ĮTEMPIŲ ZONOS ILGIO TYRIMAS DVIEJŲ SLUOKSNIŲ CILINDRINIUOSE STRYPUOSE, VEIKIANT TEMPERATŪROS POKYČIUI

R e z i u m ė

Temperatūros pokytis sluoksniuotuose konstrukcijose paprastai sukelia terminius įtempius, kurie įtakoja jų stiprumą. Šie įtempiai nėra pastovūs, tačiau kinta išilgai sluoksnio per viso elemento ilgį, ypač ties konstrukcijos pakraščiu. Sąlyginai galima išskirti dvi zonas: reguliarinę – su pastoviu (tolygiu) bei ireguliarinę – su netaisyklingu (netolygiu) įtempių pasiskirstymu. Darbe pateikiami ireguliarinės įtempių zonos ilgio tyrimo rezultatai dviejų sluoksnių pilnaviduriuose cilindriniuose strypuose veikiamuose temperatūros pokyčio. Rezultatai gauti baigtinių elementų metodu. Buvo ištirta aštuoniasdešimt viena konstrukcija su skirtingomis medžiagų tamprumo modulio, Puasono koeficiento ir sluoksnių skerspjūvio plotų vertėmis. Nustatyta, kad ireguliarinės zonos ilgis kinta maždaug nuo vienos dešimtosios iki vieno ir keturių dešimtųjų strypo išorinio diametro. Šis ilgis labiausiai priklauso nuo tamprumo modulių ir sluoksnių skerspjūvio plotų santykių. Nustatytos konstrukcijos parametrų kombinacijos, kurioms esant gaunama minimalaus/maksimalaus ilgio ireguliarinė zona. Šioms ireguliarinės zonos ilgių vertėms pateikti įtempių komponentų pasiskirstymai sluoksnių kontakte išilgai strypo ašies.

N. Partaukas, J. Bareišis

THE EXTENT OF IRREGULAR STRESS DISTRIBUTION IN A TWO-LAYER CYLINDRICAL BARS SUBJECTED TO THE CHANGE OF TEMPERATURE

S u m m a r y

The change of temperature in layered structures usually induces thermal stresses, which affect their strength. Furthermore, those stresses are not fixed along the layer, but vary especially near the edges. Consequently, two zones with a steady and variable stress distribution can be virtually distinguished. Here the results on the length of irregular stress distribution in two–layered, solid cylindrical bars subjected to change of temperature are presented. The results were obtained by means of finite element analysis. Eighty–one structures with different values of geometry and mechanical properties were analyzed. It was found that the length of irregular stress distribution zone varies approximately from one–tenth to one and a four tenths of the bar external diameter. The length depends mainly on the values of the Young's modulus and on the areas of layers cross–section. A set of design parameters which minimizes/maximizes the length of irregular stress distribution are identified. Some representative stress distributions along the axis at the layers contact are also presented.